

Pharmaceutical cocrystals prepared with a cucurbit [8]uril framework for intestine-targeted drug delivery

Jing Jia^{1,3,4}, Kan Li^{1,3,4}, Hui Xu², Bin Di^{1,3,4}, Chi Hu^{2*}, and Li-li Xu^{1,3,4*}

DOI: 10.25177/JFST.4.3.RA.509

Research

Received Date: 18th Apr 2019

Accepted Date: 10th May 2019

Published Date: 15th May 2019

Copy rights: © This is an Open access article distributed under the terms of International License.



1. Jiangsu Key Laboratory of Drug Design and Optimization, China Pharmaceutical University, Nanjing 210009, China;
2. Department of Pharmaceutical Engineering, School of Engineering, China Pharmaceutical University, Nanjing 210009, China;
3. Key Laboratory on Protein Chemistry and Structural Biology, China Pharmaceutical University, Nanjing 210009, China;
4. Key Laboratory of Drug Quality Control and Pharmacovigilance, China Pharmaceutical University, Nanjing 210009, China;

CORRESPONDENCE AUTHOR

Chi Hu: E-mail: chihu@cpu.edu.cn;

Li-li Xu: E-mail: 1620174420@cpu.edu.cn.

CITATION

Jing Jia, Kan Li, Hui Xu, Bin Di, Chi Hu, Li-li Xu, Pharmaceutical cocrystals prepared with a cucurbit[8]uril framework for intestine-targeted drug delivery(2019)SDRP Journal of Food Science & Technology 4(3)

ABSTRACT

Encapsulation of active pharmaceutical ingredients (APIs) in carrier materials for controlled delivery in the desired site is of paramount importance for optimizing the effectiveness of a therapeutic drug while minimizing its side effects. Cucurbit[8]uril (CB[8]) is herein assembled as a host framework to accommodate APIs (tryptophan, phenylalanine biapenem, and diclofenac sodium) in aqueous solution under room temperature to enhance their stability in the gastric acid and realize sustained release in the intestinal tract. Host-guest interactions were investigated by UV-vis spectroscopy while crystal structures of the supramolecular assembly were determined by single-crystal x-ray analysis, which reveals that both the CB[8] framework crystals and the API@CB[8] cocrystals belong to a monoclinic crystal system. With their aromatic rings folded inside the macrocyclic cavity of CB[8] and their alkyl chains stretching outside to interact with the carbonyl portals of CB[8] through ion-dipole interactions and hydrogen bonding, both hydrophilic and hydrophobic APIs were readily encapsulated inside the supramolecular framework. In comparison to API in its free form, an accelerated dissolution kinetic of the API@CB[8] cocrystals was observed at intestinal pH (6.8), which otherwise demonstrated a lower dissolution profile at gastric pH (1.5). With their biocompatibility confirmed by cytotoxicity test, the proposed pharmaceutical cocrystals provide a new paradigm for intestine-targeted drug delivery.

Keywords: cucurbit[8]uril; phenylalanine; single-crystal x-ray analysis; pharmaceutical cocrystal; intestine-targeted.

1. INTRODUCTION

Oral administration is widely applied in clinic and favoured by patients for its convenient portability and easy accessibility. Not all active pharmaceutical ingredients (APIs) could be taken orally, however, on account of potential problems including gastric irritation, degradation by gastric acid or enzymes, and premature release before reaching the disease site. The latter, especially, still stays as an obstacle for the treatment of irritable bowel syndrome, intestinal cancer and other intestine-associated diseases by APIs through an oral pathway[1]. Therefore, oral drug delivery systems targeting the intestinal tract, which maintain payload APIs in a biocompatible environment and release the therapeutic drugs specifically in the disease site, are receiving increasing attention.

Nowadays, various oral administration formulations aiming to target the intestinal tract have been explored. Prodrug, for example, employs linkage between carrier and the loaded drug to prevent APIs from losing activity in advance, and it has been designed to disrupt the linkage and release parent drug only in the intestinal environment[2]. This site-specific delivery is often achieved through a pH-responsive linker[3] or a functional derivative which reacts particularly with enzymes in the intestine. Another pathway often exploited is enteric coating where biocompatible polymers, such as cellulose, lipopeptide or hyaluronic acid, are mixed with APIs to prevent their degradation in the gastric acid[4]. A pH-dependent solubility of the coating polymers affords a carrier system which is insoluble and impermeable in gastric acid ($1 < \text{pH} < 3$) but dissolves promptly in neutral intestinal fluid ($5 < \text{pH} < 7$) to release APIs with adequate time to function[5].

Pharmaceutical cocrystals are new solid-state forms of old APIs with other co-existing molecules in a stoichiometric ratio, which modulate final properties without changing the pharmacological nature[6]. With the structure formed predominantly based on non-covalent interactions such as hydrogen bonding and electrostatic forces, these crystalline single-phase materials offer the intriguing possibility of exploring

different pharmaceutical properties from a single API in the quest of enhancing the final drug product.

Pharmaceutical cocrystals have been employed to improve the solubility of poorly soluble APIs. For instance, Surov and coworkers prepared a cocrystal of 1,2,4-thiadiazole with vanillic acid, which showed a 4.2 times increase in solubility compared to the parent API under optimised conditions[7]. Unlike the salification method where relatively strong acid (or base) with a $\text{p}K_a$ difference of at least two units from the weakly basic (or acidic) drugs is needed to form salts of APIs that are stable in water, pharmaceutical cocrystals designed by combining structure-matching electron donors with acceptors could overcome such restriction. Taken the extremely water-insoluble antifungal drug itraconazole for example, use of strong acids with dissociation constants below 1.7 is required in the conventional salification method, as the weakly basic piperazine ring exhibits a $\text{p}K_a$ value of 3.7. Instead, a wide range of pharmaceutically acceptable acids such as organic acid 1,4-dicarboxylic acid have been included in the formation of cocrystals of itraconazole to improve its solubility with development of the pharmaceutical cocrystal strategy[8]. Meanwhile, thermodynamic stability of pharmaceutical cocrystals is enhanced as the presence of various intermolecular and intramolecular interactions between the APIs and the surrounding co-existing molecules helps to maintain the API in the crystal format and prevent degradation such as deliquesce and oxidation when the drugs are exposed to undesirable storage conditions. For example, Lu *et al.* found that the cocrystals of berberine chloride with citric acid exhibited little water uptake under 70% relative humidity, which is the transformation humidity for pharmacopoeial grade berberine chloride[9].

Moreover, pharmaceutical cocrystals exhibit different dissolution behaviour compared to the parent drug, which could be utilised to optimise the treatment efficacy. For example, the antidiabetic drug nateglinide suffers from low dissolution rate in the upper gastrointestinal tract. Arafa *et al.* reported that cocrystallisation with sucralose increased the dissolution of nateglinide from 45.43% to 85.8% in the first 5

minutes compared to the parent drug, resulting in faster and more pronounced reduction in blood glucose level[10]. Therefore, the portfolios of pharmaceutical cocrystals offer several strategies to alter the therapeutic significance of drugs, which could be considered appropriately to match the desired pharmacokinetic response. Little efforts, however, have been devoted to intestinal targeting using the pharmaceutical cocrystal strategy.

Cucurbit[n]urils have attracted much attention for their unique host-guest interactions in acting as molecular containers with high affinity and selectivity [11]. A wide range of guest molecules, such as ammonium salts and aromatic ligands, can be encapsulated in these barrel-shaped macrocyclic hosts through non-covalent interactions including ion-dipole forces, hydrogen bonding, hydrophobic effects *et al.* Their low intrinsic cytotoxicity affords them potential applications in the pharmaceutical field. For example, Kim's group reported a 1:1 complex of cucurbit[7]uril (CB[7]) and oxaliplatin to reduce unwanted side effects of the drug[12]. Cucurbit[8]uril (CB[8]) has a larger cavity volume than CB[7] and can encapsulate two guest moieties inside its cavity simultaneously, affording more tunable and sophisticated structures for biomedical applications. CB[8] has been employed in the assembly of smart vehicles to release payload APIs upon photo- or redox-trigger after reaching the disease site[13-15]. CB[8] has also been demonstrated to bind with APIs and shift their pK_a values through ion-dipole interactions between the polar carbonyl oxygens of the host and APIs[16]. Furthermore, single-crystal formation of CB[8] has been reported on account of its various binding sites for non-covalent interactions and molecular recognition properties[17].

Here we present a new strategy to prepare pharmaceutical cocrystals, where CB[8] is employed as a crystal framework to encapsulate APIs inside its cavity. In order to explore the feasibility of this strategy, four model APIs were investigated with UV-vis spectroscopy and optical microscopy. One of the cocrystals between phenylalanine (Phe) and CB[8] was studied in detail using single-crystal X-ray analysis,

which shows that two Phe molecules were accommodated inside a single CB[8] host in the presence of various non-covalent interactions to stabilise the cocrystal structure. Release profiles of free Phe and cocrystal Phe@CB[8] were examined in stimulated gastric acid and intestinal fluid, where in the latter medium the cocrystal Phe@CB[8] showed an accelerated release with negligible cytotoxicity, making the system well-suited for the development of intestine-targeted drug formulations.

2. MATERIALS AND METHODS

2.1. Materials

Biapenem (BP) was purchased from Cubist Pharmaceuticals (U.S.). Trypsin (Trp) and Phe were purchased from Macklin Biochemical (China). Diclofenac sodium (DS) was purchased from Guangdong Tongde Pharmaceutical (China). Glycoluril and paraformaldehyde were purchased from Aladdin Biochemical Technology (China). Hydrochloric acid was purchased from Nanjing Chemical Reagents (China). Sodium hydroxide and ethanol were purchased from Sinopharm Group Chemical Reagent (China). 3-(4,5-Dimethylthiazol-2-yl)-2,5-diphenyltetrazolium bromide (MTT), dimethyl sulfoxide (DMSO), Dulbecco's modified Eagle's medium (DMEM), and trypsin were purchased from Sangon Biotech (China). Reagents were used as received without further purification. Caco-2 cells were purchased from Shanghai Institute of Biochemistry and Cell Biology, Chinese Academy of Sciences. CB[8] was prepared according to literature procedures[25,26]. Millipore 18 M Ω cm water was used in all experiments unless stated otherwise.

2.2. Methods

UV-vis spectroscopic study: Blank solutions were prepared by dissolving Trp, Phe, BP or DS to a final concentration of 0.1 M in water. Complex solutions were prepared by dissolving Trp, Phe, BP or DS to a final concentration of 0.1 M in water in the presence of 0.24 M CB[8]. In both cases, samples were sonicated for three hours and tested with UV-vis spectrometer after filtration.

Cocrystal formation: Trp@CB[8] complex was prepared by dissolving Trp and CB[8] at a molar ratio of 2 : 1. Phe@CB[8] complex was prepared by dissolving Phe and CB[8] at a molar ratio of 400 : 1. BP@CB[8] complex was prepared by dissolving BP and CB[8] at a molar ratio of 3 : 1. DS@CB[8] complex was prepared by dissolving DS and CB[8] at a molar ratio of 60 : 1. The mixtures were sonicated overnight and filtered. Subsequently, the solutions were allowed to stand at room temperature to evaporate. After about two days, cocrystals were formed for microscopy visualisation and single-crystal X-ray analysis.

Dissolution measurements: Dissolution rate was evaluated at room temperature in simulated gastroenterological conditions. Simulated gastric acid was prepared by diluting 1 M hydrochloric acid with water to a pH value of 1.5. Simulated intestinal fluid was prepared by adjusting the pH value of monopotassium phosphate to 6.8 with 0.4% (w/w) sodium hydroxide solution. Free Phe and cocrystal Phe@CB[8] were added to the simulated gastroenterological fluids by keeping the mass of the sample as 10 mg in both cases. Under a stirring rate of 100 rpm/min, 200 μ L of the sample was aspirated every three minutes and the same volume of fresh medium was supplemented the solution immediately. The collected samples were characterized with UV-vis spectrometer, and the concentration was calculated based on a calibration curve of Phe.

Cell viability assay: Cell viability in the presence of free Phe and cocrystal Phe@CB[8] was investigated by MTT assay. Caco-2 cells were seeded into a 96-well plate at a density of 5×10^3 cells per well and incubated with 5% CO₂ at 37 °C. After 12 h, the cells were treated with different concentrations of free Phe or cocrystal Phe@CB[8], followed by incubation for 24 h. Subsequently, 10 μ L of MTT (5.0 mg/mL) was added to each well and the cells were incubated for another 4 h. The medium was replaced by 100 μ L of DMSO to dissolve the resulting purple crystals. The absorbance of each well was measured at 570 nm by a microplate reader (Molecular Devices, U.S.). Each

experiment was repeated three times and the mean value was calculated.

In vivo biodistribution: Phe was determined by LC-MS/MS (QTRAP 6500+, SCIEX, US). A CORTECS C18 analytical column (100 mm \times 2.1 mm i.d., 1.6 μ m particle size, Waters, US) was used for separation. The mobile phase consisted of (A) water with 0.1% formic acid and (B) acetonitrile. The program was isocratic at a flow of 0.4 mL/min for 1 min with 40% A and 60% B. ICR male mice were used in accordance with the protocols approved by China Pharmaceutical University Laboratory Animal Center and the Animal Care and Use Committee of China Pharmaceutical University. Mice weighting 30 ± 3 g were randomly assigned (n = 3) in two groups. Group 1: A volume of 300 μ L of cocrystal Phe@CB[8] (5 mg/mL) was given orally. Group 2: A volume of 300 μ L of free Phe (5 mg/mL) was given orally. The mice were sacrificed 2 h after treatment. The stomach and intestine were collected and processed to analyze the presence of Phe. Tissues and organs were separated, suspended in PBS buffer (pH 7.4) with a weight ratio of 1:9, and subjected to a bead-based homogenizer (TC-Metero, Topscien, China). After centrifugation (10,000 rpm, 5 min), 700 μ L of the upper layer supernatant was collected, filtered using a 0.22 μ m syringe filter and injected into machine for analysis.

Statistics: Information on statistical tests is present in all figure legends. Two-tailed t tests were used when comparing two groups, as indicated in figure legends. All data sets were assumed to fit a normal distribution, and all graphs show mean and error bars represent standard error of the mean (SEM). All statistical analysis was performed using SPSS (Statistical Product and Service Solutions) software.

3. RESULTS AND DISCUSSION

3.1 Inclusion complex of API@CB[8]

Four model APIs were investigated in this work, *i.e.*, Trp, Phe, BP and DS, and their structures are shown in Figure 1. Trp[18] and Phe[19] have been reported to form host-guest complexes with CB[8], the crystal structures of which have not been elucidated yet. BP is a synthetic antibiotic widely used to treat infec-

tions, and DS is a common drug to treat inflammation in clinic.

Supramolecular interactions between the four model APIs and the macrocyclic host CB[8] were firstly investigated by UV-vis spectroscopy. As CB[8] itself does not exhibit any significant absorption between 200 to 400 nm, where API often shows observable signal due to π - π^* transition in its aromatic ring, change in the electron distribution in API on account of the formation of host-guest complexation could be readily detected. As shown in Figure 1, change in the peak intensity of APIs was observed upon complexation with CB[8], demonstrating decrease in the absorption value. While Trp and Phe showed minor change in the absorption value after being accommodated inside CB[8], BP and DS exhibited quite pronounced decrease in the maximum absorption peak upon complex formation. Experiments were repeated six times using separately prepared samples, and in each time the same minor change in absorbance was recorded for Phe and Trp, ensuring what we observed was not error propagated from impurities, preparation, etc.

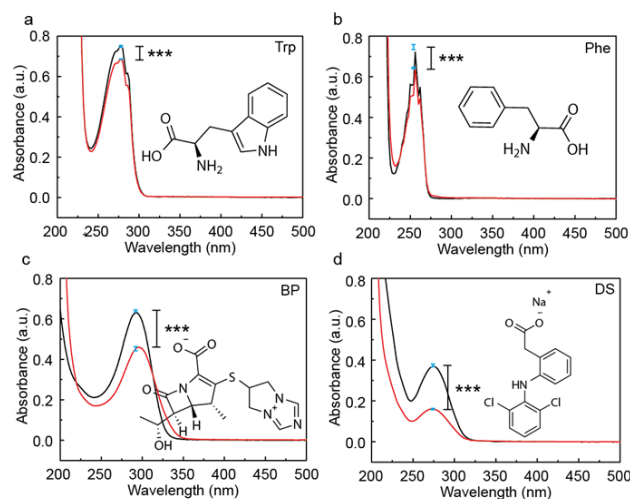


Figure 1. UV-vis spectra of four model APIs (a) Trp, (b) Phe, (c) BP and (d) DS. The black line represents free API, and the red line represents API@CB[8] after complex formation. Significance was measured by two-tailed t test. *** $p < 0.001$, ** $p < 0.01$, * $p < 0.05$.

3.2 Cocrystal of API@CB[8]

Crystal structure of CB[8] has been elucidated[20]. Here we employ this crystal framework in the preparation of pharmaceutical cocrystals on account of the presence of host cavities to accommodate various APIs through the formation of inclusion complex API@CB[8]. Cocrystals of CB[8] with four model APIs (Trp, Phe, BP and DS) were successfully prepared, and their morphology were visualised by optical microscopy, as shown in Figure 2. Notably, the cocrystals were all fabricated under mild conditions in aqueous solution and room temperature.

Transparent, rhombus-shaped cocrystals of Trp@CB[8] were observed as shown in Figure 2a, which were about 120 μm in the longest side and 80 μm in the shortest side, respectively. Their crystal data, however, was not successfully obtained by single-crystal X-ray analysis. This is likely on account of the dynamic host-guest association and dissociation, which result in a compromised crystal quality. Small pieces of ununiform solids without a definite shape were also present, which seem to be broken or immature crystals, even under the optimised conditions in our experiments. Rod-shaped cocrystals of Phe@CB were observed with sharp edges and a transparent colour, as shown in Figure 2b. Unlike the monolayer, sheet-like cocrystals of Trp@CB, cocrystals of Phe@CB were three-dimensional in shape exhibiting different crystal faces, as shown by the dark edges on both sides along the axis of the rod-shaped crystal in Figure 2b. Moreover, size of the Phe@CB cocrystals is approximately 280 μm in length and 90 μm in diameter, which is relatively large and suitable for single-crystal X-ray analysis.

Tiny microcrystals of BP@CB[8] with a size of approximately 20 μm in diameter were visualised as shown in Figure 2c. Cocrystals with different shapes were observed for DS@CB[8]. As shown in Figure 2d, block-shaped cocrystals with a size of 70 μm in length and 18 μm in width were observed together with microcrystals, which were around 35 μm in diameter. It was difficult to distinguish the colour of these cocrystals from their yellowish background which was the colour of the mother liquid. From our

experience, a more transparent colour of the cocrystal often indicates more stable structures.

It is noteworthy that these cocrystals are most stable in their mother liquor. While their crystal shapes are well maintained for at least one week in the mother liquor, they are prone to crack in several hours once redispersed in water. This phenomenon is quite predictable as the host-guest complexation of CB[8] is a reversible process driven by the concentrations of its individual components, *i.e.*, host and the guest moieties. The concentration balance required for cocrystal formation is maintained in the mother liquor, but disturbed otherwise, resulting in cracking and damage of the crystal structure.

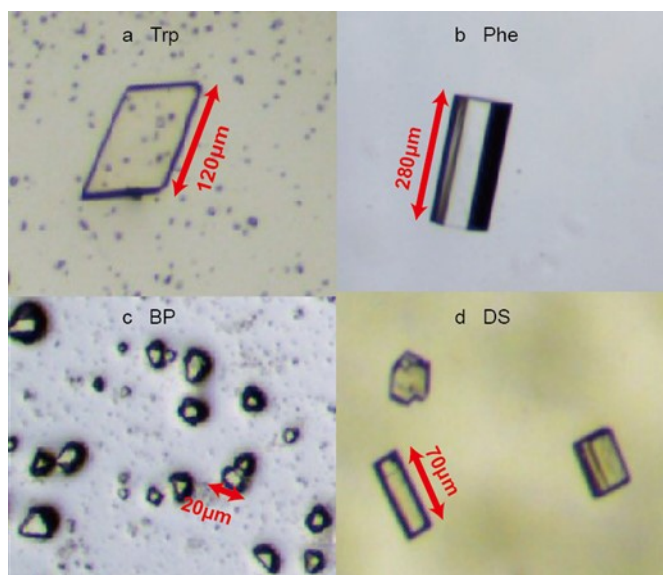


Figure 2. Microscopy images of cocrystals: (a) Trp@CB[8], (b) Phe@CB[8], (c) BP@CB[8] and (d) DS@CB[8].

3.3 Single-crystal X-ray analysis

The four model APIs were incorporated into the crystal framework of CB[8] and pharmaceutical cocrystals prepared as visualised by optical microscopy. However, only the cocrystal of Phe@CB was successfully analysed by single-crystal X-ray analysis and crystal data obtained on account of its relatively large size and stable structure. Cocrystal Phe@CB[8] has an empirical formula of $C_{66}H_{87}N_{34}O_{43}$, and its crystal data reveals a monoclinic structure with P21 space group, containing two sets of Phe@CB[8]

complex in each crystal unit. Detailed information regarding the crystal structure of Phe@CB[8] is listed in Table 1.

Table 1. Crystallographic data for cocrystal Phe@CB[8]

Identification Code	Phe@CB[8]
Empirical formula	$C_{66}H_{87}N_{34}O_{43}$
Formula Weight	2044.69
Temperature/K	100.00(10)
Crystal system	Monoclinic
Space group	P21
a/Å	13.5462(7)
b/Å	13.5049(11)
c/Å	26.0684(13)
α /°	90
β /°	93.145(5)
γ /°	90
Volume/Å ³	4761.8(5)
Z	2
Crystal size/mm ³	0.13 x 0.11 x 0.09
Reflections collected	20844
Independent reflections	14732[Rint = 0.0674, Rsigma = 0.1218]
Goodness-of-fit on F2	1.066
Final R indexes[I \geq 2 σ (I)]	R1 = 0.0940, wR2 = 0.2285
CCDC deposit number	1877041

As shown in Figure 3a, benzene ring of the Phe molecule was encapsulated into the cavity of the macrocyclic host while its ammonio carboxylate group resided outside the portal area of CB[8], forming the inclusion complex Phe@CB[8]. Packing diagram of the cocrystal in the c^* -axis is demonstrated in Figure 3b, where adjacent Phe@CB[8] complex units exhibit a zigzag special arrangement, affording an ordered three-dimensional structure and facilitating the formation of robust cocrystals. Two-dimensional diagram and three-dimensional structure of CB[8] and Phe molecules before complex formation are presented in Figure 3c and d for clearance.

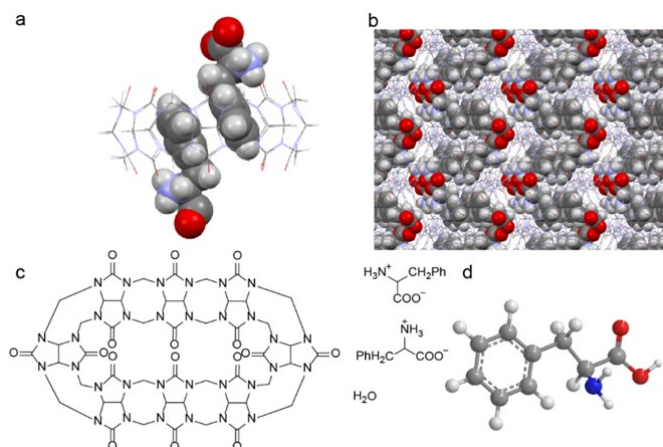


Figure 3. X-ray crystal structure of Phe@CB[8] co-crystals: (a) a single complex unit, where Phe is presented in spacefill model and CB[8] in wireframe model, and (b) packing diagram in c^* -axis. Structures of CB[8] and Phe molecules are illustrated in (c) two-dimensional diagram, and (d) three-dimensional structure for clearance. Atoms are presented as C: gray, N: blue, O: red, H: white.

Detailed interaction forces are calculated by Mercury 3.5 as shown in Figure 4, which provide information regarding the host-guest complexation and co-crystal formation[21]. As shown in Figure 4a, a N–H...O distance of 2.549 Å was calculated between the amino group of Phe and a carbonyl oxygen of CB[8], while a N–H...O distance of 2.091 Å and 2.721 Å was observed between the second Phe and two separate carbonyl oxygen atoms of CB[8]. These three intermolecular forces are within the range of hydrogen bonding[22], which together afford an energetically optimised host-guest network. Moreover, the crystal structure of Phe@CB[8] clearly showed two parallel Phe molecules inserted almost vertically into the host cavity of CB[8]. Distance between the centres of two benzene rings is 3.826 Å (Figure 4b), which corresponds to a face-to-face π - π stacking interaction[23].

Meanwhile, water molecules around the inclusion complex form a sophisticated network of hydrogen bonding to stabilise the supramolecular structure (Figure 4c). Short contact (< sum of Van der Waals forces) also exists between the encapsulated Phe guests, the inner wall of CB[8] and the surrounding

solvent molecules as calculated by Mercury 3.5, which plays an important role in stabilising the inclusion geometry of Phe@CB[8] (Figure 4d). Together, the presence of these intermolecular forces between the guest and host molecules facilitates the encapsulation of Phe into the crystal framework of CB[8] and the formation of a robust co-crystal.

3.4 pH-dependent release profiles

On the basis of these premises, release kinetics of the two different formulation strategies, *i.e.*, free Phe and co-crystal Phe@CB[8], were investigated. Time-dependent release test was carried out in simulated gastric acid (pH 1.5) and intestinal fluid (pH 6.8), which are the two major digestion environments *in vivo*. Release characteristics were firstly evaluated by naked eyes, where equal quantities of co-crystal Phe@CB[8] were dispersed in stimulated gastric acid and intestinal fluid, respectively (see Figure S6 in Supporting Information). After 10 min of stirring under 100 rpm, less solids were left in the stimulated intestinal fluid compared to that in the stimulated gastric acid, suggesting that co-crystal Phe@CB[8] is more stable in acidic environment.

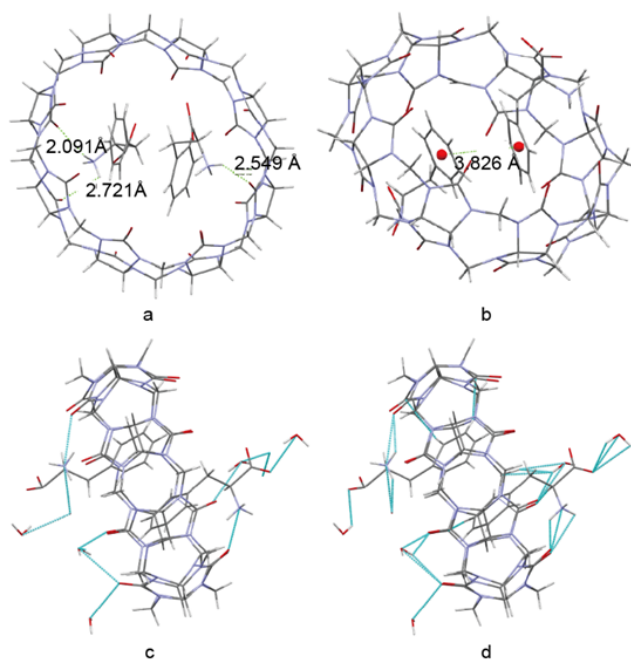


Figure 4. (a) Hydrogen bonding between Phe and the host framework of CB[8], (b) π - π stacking between two Phe moieties encapsulated in a single CB[8] host, (c) all hydrogen bonding, and (d) short contact

(< sum of Van der Waals forces) in the whole cocrystal.

Release of Phe from free Phe powders and encapsulated Phe@CB[8] cocrystals were readily monitored by UV-vis spectroscopy at 254 nm, which corresponds to π - π^* transition in the aromatic ring. It is noteworthy that release of Phe from both of the two different formulations could be quantified at this wavelength using the same calibration curve as negligible change in absorption was observed for Phe before and after its complexation with CB[8] (Figure 1b). Upon dispersion in the stimulated gastric acid, both free Phe and cocrystal Phe@CB[8] firstly showed rapid dissolution with a sharp gradient (phase 1), which then slowed down and reached a plateau (phase 2). As shown in Figure 5, phase 1 is mainly due to the dissolution of Phe molecules near the surface of the powder or cocrystal, which are readily dissolved into the solvent system. Subsequently, dissolution rate of free Phe and cocrystal Phe@CB[8] slows down for different reasons during phase 2. In the case of free powder, released Phe molecules form a concentrated layer around the remaining solids, which need to diffuse away before further dissolution could effectively take place. For cocrystal Phe@CB[8], water molecules need to penetrate into the void space inside the crystal skeleton, leading to collapse of the crystal framework and release of the encapsulated Phe.

As shown in Figure 5a, an accelerated release from free Phe in comparison to cocrystal Phe@CB[8] was observed under pH 1.5, presumably on account of the protonation of the amino groups of Phe in the stimulated gastric acid, which facilitates dissolution and diffusion of the free powder. On the contrary, cocrystal Phe@CB[8] exhibited an impeded release kinetics likely due to the presence of multiple intermolecular interactions within the cocrystal framework, which stabilized the crystal structure. Upon exposure to the stimulated intestinal fluid at pH 6.8, however, entirely different release profiles were observed as shown in Figure 5b, where the release rate of cocrystal Phe@CB[8] was substantially more pronounced than free Phe. This is likely because of the effect of CB[8]

as a solubiliser to increase the solubility of hydrophobic APIs. Based on its decreased release under pH 1.5 and increased release under pH 6.8, cocrystal Phe@CB[8] can effectively maintain and protect the API through the gastric environment until it reaches the intestinal tract, affording a potential colon-targeting formulation strategy.

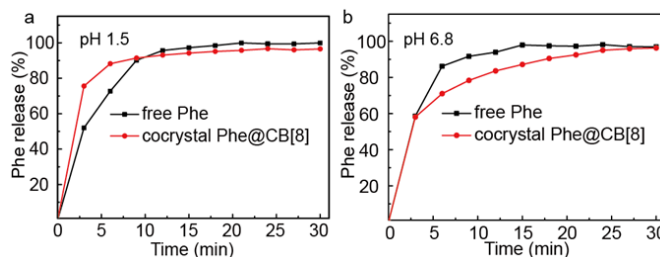


Figure 5. Release profiles for free Phe and cocrystal Phe@CB[8] in (a) simulated gastric fluid at pH 1.5, and (b) simulated intestinal fluid at pH 6.8.

3.5 Biocompatibility assay

Low *in vitro* and *in vivo* toxicity of CB[8] has been demonstrated in literature[24], here we further examined the biocompatibility of CB[8]-based pharmaceutical cocrystals on Caco-2 cells, which are derived from a colon carcinoma but resemble the enterocytes lining the intestine. Different concentrations of free Phe or cocrystal Phe@CB[8] were added in the culture medium of Caco-2 cells, the viability of which was then measured after 24 h using the MTT method. As shown in Figure 6, as the concentration of cocrystal Phe@CB[8] increased from 0.5 to 500 μ g/mL, viability of Caco-2 cells was not affected and moderate cell proliferation was observed. Interestingly, the highest cell viability was obtained when the highest concentration of free Phe or cocrystal Phe@CB[8], *i.e.*, 500 μ g/mL was added to the culture medium, presumably on account of the nutritional effects of Phe. Moreover, no significant difference in cell viability was observed between the two formulation strategies. The results indicate that pharmaceutical cocrystals prepared using the crystal framework of CB[8] exhibit no apparent *in vitro* cytotoxicity, demonstrating the potential of utilising this supramolecular approach for the development of novel pharmaceutical cocrystals targeting the intestinal tract.

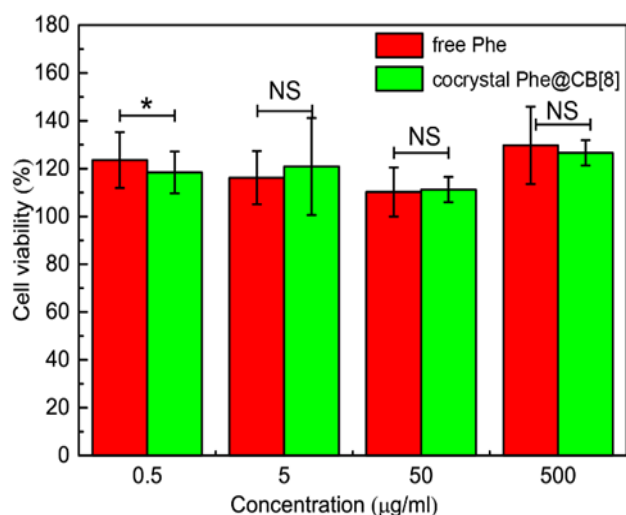


Figure 6. Viability of Caco-2 cells treated with different concentrations of free Phe or cocystal Phe@CB[8]. Significance was measured by two-tailed t test. * $p = 0.049$.

3.6 In vivo biodistribution

To prove the enhanced accumulation of API in the intestinal tract from the cocystal Phe@CB[8], in vivo biodistribution studies were carried out. For this purpose, male ICR mice were divided into two groups. Mice in group 1 were treated with 300 µL of cocystal Phe@CB[8] (5 mg/mL), and mice in group 2 were treated with 300 µL of free Phe (5 mg/mL). The presence of Phe in the stomach and intestine was also evaluated. As could be seen in Figure 7A, subjects in group 1 showed lower Phe levels in the stomach in comparison to mice in group 2. On the contrary, the levels of the API in the intestine (Figure 7B) were higher in mice treated with cocystal Phe@CB[8] compared to levels observed in the mice treated with free Phe. The remarkable concentration of Phe in intestine for subjects treated with cocystal Phe@CB[8] strongly suggests the intestine-targeted delivery properties of the proposed pharmaceutical cocystal strategy.

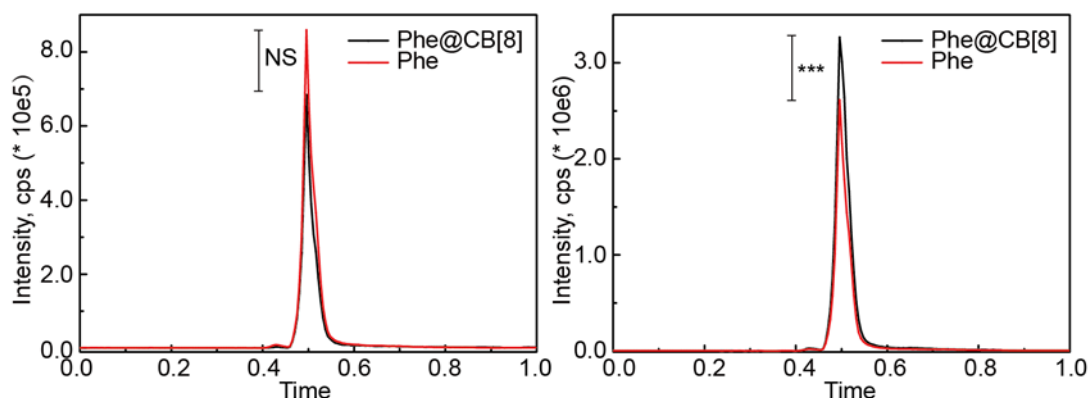


Figure 7. In vivo biodistribution of cocystal Phe@CB[8] and free Phe in the stomach (A) and in the intestinal tract (B). Significance was measured by two-tailed t test to give *** $p < 0.001$.

4. Conclusions

In summary, a novel method to prepare pharmaceutical cocystals has been developed by exploiting the heterogeneous guest inclusion capability of CB[8] to encapsulate APIs inside the crystal framework of CB[8] for colon-targeted drug delivery, which is normally not achievable with pharmaceutical cocystals prepared using the standard techniques. This approach provides a method with minimal sample preparation to avoid pre-mature release of APIs in the gastric acid and obtain drug delivery specifically in the colon

tract. In this initial study, we have demonstrated the concept using Phe, but the applicability of this facile and robust method can be easily extended to drug formulations with a variety of other APIs. Formation of inclusion complex in solution was confirmed by UV-vis spectroscopy, and successful preparation of Phe@CB[8] cocystals was visualized by optical microscope as well as single-crystal X-ray analysis. The prepared Phe@CB[8] cocystals displayed an acceler-

ated release profile in the stimulated intestinal fluid in comparison to the gastric acid, and exhibited good biocompatibility in in vitro cytotoxic assessment using Caco-2 cells. Therefore, these self-assembled pharmaceutical crystals by CB[8] in a controlled and reproducible manner provide a convenient platform for the targeted drug delivery in colon tract and offer major advantages over conventional cocrystal systems.

Author Contributions: Conceptualization, Chi Hu and Lili Xu; Data curation, Jing Jia, Kan Li and Hui Xu; Formal analysis, Jing Jia; Funding acquisition, Bin Di, Chi Hu and Lili Xu; Methodology, Kan Li; Validation, Hui Xu; Writing – original draft, Jing Jia and Chi Hu; Writing – review & editing, Bin Di and Lili Xu.

Funding: This work was financially supported by the National Natural Science Foundation of China (NO. 81573386, 81803354), Excellent Science and Technology Innovation Team Projects of Jiangsu Province Universities in 2017 and the Fundamental Research Funds for the Central Universities (NO. 2016ZPT005), Natural Science Foundation of Jiangsu Province of China (NO. BK20180564).

Acknowledgments: We also thank the staffs from BL17B at Shanghai Synchrotron Radiation Facility, for assistance during data collection.

Abbreviations

APIs	Active pharmaceutical ingredients
CB[8]	Cucurbit[8]uril
CB[7]	Cucurbit[7]uril
Phe	Phenylalanine
BP	Biapenem
Trp	Trypsin
DS	Diclofenac sodium
MTT	3-(4,5-Dimethylthiazol-2-yl)-2,5-diphenyltetrazolium bromide
DMSO	Dimethyl sulfoxide
DMEM	Dulbecco's modified Eagle's medium

REFERENCES

- [1] Lautenschläger, C.; Schmidt, C.; Fischer, D.; Stallmach, A. Drug delivery strategies in the therapy of inflammatory bowel disease. *Adv. Drug Deliver. Rev.* 2014, 71, 58-76. PMID:24157534 [View Article](#) [PubMed/NCBI](#)
- [2] Jain, S.K.; Anekant, J. Target-specific drug release to the colon. *Expert Opin. Drug Delivery* 2008, 5, 483. PMID:18491977 [View Article](#) [PubMed/NCBI](#)
- [3] Butt, A.; Jabeen, S.; Nisar, N.; Islam, A.; Gull, N.; Iqbal, S.; Khan, S.; Yameen, B. Controlled release of cephadrine by biopolymers based target specific crosslinked hydrogels. *Int. J. Biol. Macromol.* 2019, 121, 104-112. PMID:30291928 [View Article](#) [PubMed/NCBI](#)
- [4] Xing, X.; Zhao, X.; Ding, J.; Liu, D.; Qi, G. Enteric-coated insulin microparticles delivered by lipopeptides of iturin and surfactin. *Drug Deliv.* 2018, 25, 23-34. PMID:29226733 [View Article](#) [PubMed/NCBI](#)
- [5] Cox, D.; Maree, A.O.; Dooley, M.; Conroy, R.; Byrne, M.F.; Fitzgerald, D.J. Effect of enteric coating on antiplatelet activity of low-dose aspirin in healthy volunteers. *Stroke* 2006, 37, 2153. PMID:16794200 [View Article](#) [PubMed/NCBI](#)
- [6] Shaikh, R.; Singh, R.; Walker, G.; Croker, D. Pharmaceutical cocrystal drug products: an outlook on product development. *Trends Pharmacol. Sci.* 2018, 39, 1033-1048. PMID:30376967 [View Article](#) [PubMed/NCBI](#)
- [7] Surov, A.O.; Volkova, T.V.; Churakov, A.V.; Proshin, A.N.; Terekhova, I.V.; Perlovich, G.L. Cocrystal formation, crystal structure, solubility and permeability studies for novel 1,2,4-thiadiazole derivative as a potent neuroprotector. *Eur. J. Pharm. Sci.* 2017, 109, 31. PMID:28756204 [View Article](#) [PubMed/NCBI](#)
- [8] Remenar, J.F.; Morissette, S.L.; Peterson, M.L.; Moulton, B.; MacPhee, J.M.; Guzmán, H.R.; Almarsson, Ö. Crystal engineering of novel cocrystals of a triazole drug with 1,4-dicarboxylic acids. *J. Am. Chem. Soc.* 2003, 125, 8456-8457. PMID:12848550 [View Article](#) [PubMed/NCBI](#)
- [9] Lu, Q.; Dun, J.; Chen, J.M.; Liu, S.; Sun, C.C. Improving solid-state properties of berberine chloride through forming a salt cocrystal with citric acid. *Int. J. Pharm.* 2019, 554, 14-20. PMID:30385378 [View Article](#) [PubMed/NCBI](#)
- [10] Arafa, M.F.; El-Gizawy, S.A.; Osman, M.A.; Maghraby, G.M.E. Co-crystallization for en-

- hanced dissolution rate of nateglinide: in vitro and in vivo evaluation. *J. Drug Delivery Sci. Technol.* 2017, 38, 9-17. [View Article](#)
- [11] Huang, W.H.; Liu, S.; Isaacs, L. Modern supramolecular chemistry: strategies for macrocycle synthesis; François Diederich, P.J.S., Rik R. Tykwinski Ed. Wiley: Weinheim, 2008; 113-142.
- [12] Young Jin, J.; Soo-Young, K.; Young Ho, K.; Shigeru, S.; Kentaro, Y.; Kimoon, K. Novel molecular drug carrier: encapsulation of oxaliplatin in cucurbit[7]uril and its effects on stability and reactivity of the drug. *Org. Biomol. Chem.* 2005, 3, 2122-2125. PMID:15917899 [View Article](#) [PubMed/NCBI](#)
- [13] Zhao, J.; Chen, C.; Li, D.; Liu, X.; Wang, H.; Jin, Q.; Ji, J. Biocompatible and biodegradable supramolecular assemblies formed with cucurbit[8]uril as a smart platform for reduction-triggered release of doxorubicin. *Polym. Chem.* 2014, 5, 1843-1847. [View Article](#)
- [14] Hu, C.; Ma, N.; Li, F.; Fang, Y.; Liu, Y.; Zhao, L.; Qiao, S.; Li, X.; Jiang, X.; Li, T. Cucurbit [8]uril-based giant supramolecular vesicles: highly stable, versatile carriers for photoresponsive and targeted drug delivery. *ACS Appl. Mater. Interfaces* 2018, 10, 4603-4613. PMID:29333854 [View Article](#) [PubMed/NCBI](#)
- [15] Xu, Q.; Wang, J.L.; Luo, Y.L.; Li, J.J.; Wang, K.R.; Li, X.L. Host-guest interactions and controllable capture and release of proteins based on cationic perylene bisimides. *Chem. Commun.* 2017, 53, 2241-2244. PMID:28144645 [View Article](#) [PubMed/NCBI](#)
- [16] Huang, Y.; Hu, Q.H.; Song, G.X.; Tao, Z.; Xue, S.F.; Zhu, Q.J.; Zhou, Q.; Wei, G. Cucurbit [7,8]urils binding to gefitinib and the effect of complex formation on the solubility and dissolution rate of the drug. *RSC Adv.* 2013, 4, 3348-3354. [View Article](#)
- [17] Mitkina, T.V.; Sokolov, M.N.; Naumov, D.Y.; Kuratieva, N.V.; And, O.A.G.; Fedin, V.P. Complex within a molecular container: selective encapsulation of trans-[Co(en)2Cl2]⁺ into cucurbit[8]uril and influence of inclusion on guest's properties. *Inorg. Chem.* 2006, 45, 6950-6955. PMID:16903754 [View Article](#) [PubMed/NCBI](#)
- [18] Sankaran, S.; Cavatorta, E.; Huskens, J.; Jonkheijm, P. Cell adhesion on RGD-displaying knottins with varying numbers of tryptophan amino acids to tune the affinity for assembly on cucurbit[8]uril surfaces. *Langmuir* 2017, 33, 8813-8820. PMID:28514856 [View Article](#) [PubMed/NCBI](#)
- [19] De Vink, P.J.; Briels, J.M.; Schrader, T.; Milroy, L.G. A binary bivalent supramolecular assembly platform based on cucurbit[8]uril and dimeric adapter protein 14-3-3. 2017, 56, 8998-9002. PMID:28510303 [View Article](#) [PubMed/NCBI](#)
- [20] Ayhan, M.M.; Karoui, H.; Hardy, M.; Rockenbauer, A.; Charles, L.; Rosas, R.; Udachin, K.; Tordo, P.; Bardelang, D.; Ouari, O. Comprehensive synthesis of monohydroxy-cucurbit[n]urils (n = 5, 6, 7, 8): high purity and high conversions. *J. Am. Chem. Soc.* 2015, 137, 10238-10245. PMID:26197228 [View Article](#) [PubMed/NCBI](#)
- [21] Macrae, C.F.; Bruno, I.J.; Chisholm, J.A.; Edgington, P.R.; McCabe, P.; Pidcock, E.; Rodriguez-Monge, L.; Taylor, R.; Streek, J.v.d.; Wood, P.A. Mercury CSD 2.0-new features for the visualization and investigation of crystal structures. *J. Appl. Crystallogr.* 2008, 41, 466-470. [View Article](#)
- [22] Sodupe, M.; Oliva, A.; Bertran, J. Theoretical study of the ionization of the H₂O-H₂O, NH₃-H₂O, and FH-H₂O hydrogen-bonded molecules. *J. Am. Chem. Soc.* 1994, 116, 8249-8258. [View Article](#)
- [23] Głównka, M.L.; Martynowski, D.; Kozłowska, K. Stacking of six-membered aromatic rings in crystals. *J. Mol. Struct.* 1999, 474, 81-89. 00562-6 [View Article](#)
- [24] Rowland, M.J.; Parkins, C.C.; McAbee, J.H.; Kolb, A.K.; Hein, R.; Loh, X.J.; Watts, C.; Scherman, O.A. An adherent tissue-inspired hydrogel delivery vehicle utilised in primary human glioma models. *Biomaterials* 2018, 179, 199-208. PMID:30037456 [View Article](#) [PubMed/NCBI](#)
- [25] Kim, J.; Jung, I.S.; Kim, S.Y.; Lee, E.; Kang, J.K.; Sakamoto, S.; Yamaguchi, K.; Kim, K. New cucurbituril homologues: syntheses, isolation, characterization, and X-ray crystal structures of cucurbit[n]uril (n = 5, 7, and 8). *J. Am. Chem. Soc.* 2000, 122, 540-541. [View Article](#) [PubMed/NCBI](#)
- [26] Day, A.; Arnold, A.P.; Blanch, R.J.; Snushall, B. Controlling factors in the synthesis of cucurbituril and its homologues. *J. Org. Chem.* 2001, 66, 8094. PMID:11722210 [View Article](#) [PubMed/NCBI](#)